ISSN 2278-3091
Volume 10, No.2, March - April 2021
International Journal of Advanced Trends in Computer Science and Engineering
Available Online at http://www.warse.org/IJATCSE/static/pdf/file/ijatcse1351022021.pdf
https://doi.org/10.30534/ijatcse/2021/1351022021

Improve communication network issues for multi UAV

Ammar Oad[1*], Pinial Khan Butt[2], Ghulam Mujtaba Khushk[2],Aneel Oad[3],Huang lei[1], Mansoor Ahmed Khuhro[4], Sajida Raz Bhutto[3]

[1] Faculty of Information Engineering, Shaoyang University, Shaoyang 422000, China,
[*]ammar_2k309@yahoo.com, 87431539@qq.com
[2] Information Technology Center, Sindh Agriculture University Tando Jam 70060, Pakistan, pinial@sau.edu.pk, khushk.ghulammujtaba@gmail.com
[3]Information Engineering, Central South University, Changsha, Hunan, China, oad_aneel@yahoo.com, sajida.raz@muetkhp.edu.pk
[4] Department of Computer Science, Sindh Madressatul-Islam University (SMIU), Karachi, Sindh, Pakistan, 74000, makhuhro@smiu.edu.pk

ABSTRACT

In this paper, we address the problems of power efficiency, real-time routing, and rate allocation in flying ad-hoc networks (FANETs). The study designed a cross-layer optimization framework with delay constraints to solve the proposed problems and then used Lagrangian relaxation and dual decomposition methods to decompose the joint optimization problem into several lower complexity sub-problems. Moreover, Case model 3 is employed that allows each relay node to complete the optimization of different sub-problems through local information. The results show that the proposed algorithm can effectively increase the network throughput and reduce the packet-timeout ratio and power efficiency.

Key words: Unmanned aerial vehicle, real-time routing, Flying Ad hoc Networks, mobile ad hoc network, power efficiency.

1. INTRODUCTION

In recent years, unmanned aerial vehicles (UAVs) have been increasingly used to collect data due to their higher spatial and temporal resolutions [1]. Generally, a single-UAV system is used owing to its flexibility, easy installation, and scalability [2]. However, the single-UAV framework cannot be generalized to further applications because of its simple functions and minimal coverage. To overcome this shortcoming and extend the application range, the multi-UAV system can be established by combining different singleUAVs [3]. A link between the single-UAV and the base station may disconnect in the multi-UAV system due to the limited communication radius. This limitation reduces the application range of the multi-UAV system. An alternative solution is to establish an ad hoc mode network between the different UAVs, called the Flying Ad Hoc Networks (FANET). In FANET, each UAV can communicate with the base station through single-hop or multi-hop mode, and each UAV can be used as a source node. It can also be used as a relay node to help other UAVs transfer data packets. Compared with a single-UAV system, FANET has better flexibility and scalability. It allows UAVs to choose different communication modes according to the actual needs. It also enables UAVs to fly freely within a specific range to expand the scope of monitoring. Although FANET can overcome the limitations of the single-UAV system, it also faces some challenges. Among them, the main three problems are real-time routing, rate allocation, and power control. FANET has higher mobility and spatial dimensions, resulting in the failure of the pre-established path be-tween the source node and the destination node [4]. Therefore, in the FANET, the connection time between nodes should be considered for the routing problem. Real-time routing requires each data packet to reach the destination node within the delay constraint. Thus, one of the research objectives of the present study is designing an algorithm that meets the characteristics and requirements of FANET and delay constraint simultaneously. UAVs work in three dimensional space and the links established between them are more susceptible to interference from other wireless signals, which in turn, influences their performance. This study also focuses on finding an appropriate way to choose the transmission power that can reduce the interference between signals and ensure the reliability of the transmission. A precise interference model enables the transmitter to choose a more suitable relay node and ensures that each data packet is delivered to the destination node with a higher probability. In FANET, the link capacity between UAVs is restricted by physical channels. The transmission rate of each UAV is limited to a specific range. If the range is exceeded, data packets cannot be received correctly. The upper bound of the transmission rate is determined by the transmission power and interference

signals. Therefore, it is necessary to select an appropriate transmission power and transmission rate to ensure the reliability of end-to-end transmission and meet the requirements of real-time routing. In the FANET, the centralized optimization method does not work correctly due to the rapid change of the link state. The distributed approach works more efficiently since it allows each UAV to only exchange information with its neighbors. First, to implement the distributed method, use the Lagrangian relaxation method to transform the centralized problem into a distributed problem and then use the primitive-dual decomposition method to de-compose the global problem into several smaller sub-problems [5]. Due to the unreliability of the wireless link, the loss of data packets during the transmission process can easily cause some relay nodes to be unable to update net-work parameters based on current information. The traditional synchronization optimization method requires all nodes to update the parameters according to the newly received data packets simultaneously [6], which is difficult to achieve in an unreliable communication environment. The asynchronous optimization method allows the node to update the parameters using the recently saved information when it does not receive a new data packet [7]. Therefore, the asynchronous optimization method can solve the problem that some nodes cannot update the parameter normally due to the loss of data packets. The present study has two main contributions. First, the study proposes a cross-layer optimization framework with delay constraints by using Lagrangian relaxation and primitive-dual decomposition techniques to divide the problem into several polynomial-time solvable sub-problems. Second, the study also proposes a delay-aware distributed optimization algorithm based on the asynchronous update. Each relay node uses only local information to update the original and dual variables to achieve an optimal solution.

2. RELATED WORK

Previous studies [8, 9] have explored the routing problem in FANET. They designed routing algorithms by con-side ring different network models and parameters to meet the needs of FANET. However, the algorithm cannot account for the relatively large limitations of routing optimization. Qu et al. [10] proposed a cross-layer optimization algorithm that satisfies the end-to-end delay constraint to ensure that the physical layer, MAC Layer, and net-work layer can interact well in real-time wireless networks. Wu et al. [11] proposed two simple distributed strategies, in which the optimization operation is completed at each node without requiring coordination between nodes. Rukmani et al. [12] suggested a high-capacity cross-layer optimization strategy based on interference management. They considered the interference elimination and area division methods in the multi-hop and multi-base station scenario, and to provide greater throughput routing based on small hops or multi-time slice allocation is designed. The optimization method introduced above cannot be directly applied to FANET since, in the FANET, the link status changes rapidly. The high-speed mobility of UAV leads to rapid changes in FANET's network topology and unreliable links. These characteristics result in the failure of the pre-established path between the source node and the destination node. Studies [13, 14] have shown that synchronous optimization methods require all nodes to timely update their network parameters. This operation may result in communication overhead which is inappropriate in FANET. However, asynchronous optimization methods do not require collaboration between nodes. Each node can use old information to update the current parameters. These methods can ensure the convergence and optimization performance of the algorithm in scenarios with significant delays and poor communication quality. The advantages of the asynchronous method make it valuable for different scenarios, including smart grid and communication networks [15, 16]. These methods start from different perspectives, such as the nature of the objective function and the algorithm's convergence. The algorithm proposed in this paper only needs some nodes to up-date their own parameters during each iteration. Regarding the problem of resource allocation in the coded wireless network multicast scene, Jiang et al. [17] proposed a cross-layer design scheme that jointly optimizes the end-to-end transmission layer rate, link capacity, and average power consumption, combined with the idea of asynchronous optimization. FANET is a self-organizing network. All nodes in the network are homogeneous and fast-moving. These mobile nodes constitute a randomly changing network topology. Given the limitations of the above methods, combined with the idea of asynchronous updates, considering the end-to-end delay and interference at each relay node, this paper proposes a distributed cross-layer optimization method to solve the proposed problem.

3.FANET NETWORK MODEL AND PROBLEM DESCRIPTION

3.1 FANET NETWORK MODEL

Assuming that UAVs are evenly distributed in a specific area, each UAV can be used as a source node and a relay node simultaneously, while the ground base station can only be used as a destination node. All UAVs can fly freely in the area, while the coordinates of the base station are fixed. UAVs can transmit data to the base stations through one-hop or multi-hop transmission mode, as shown in Figure 1. The network topology of FANET can be represented through the undirected graph, which is as follow:

$$G = (M, N) \qquad (1)$$

Where M represents the collection of all UAVs, and N represents the collection of all links in the network (the dotted line between UAVs in Figure 1). To simplify the notation, node e represents the e^{th} UAV. The signal transmitted by node e can be received by node a, then $a \in V_e^t$, where $V_e^t = \{a \mid (e, a) \in N\}$ is the set of neighbors of node e at time t and (e, a) shows the sequence of the objects.

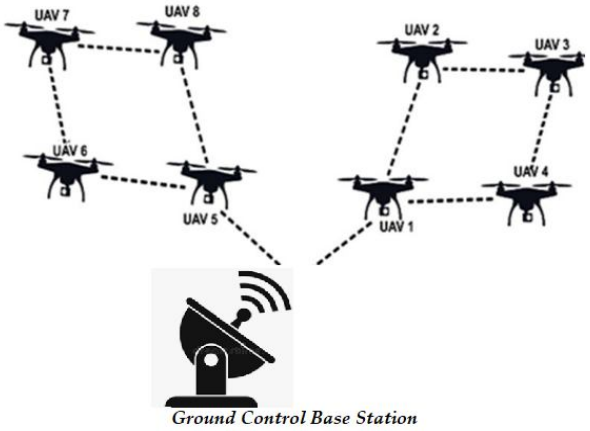

Figure 1 FANET network model.

3.1.1 INTERFERENCE OUTAGE PROBABILITY

To improve transmission efficiency and reduce network resources and delay consumption, each relay node needs to evaluate the quality of the link with its neighbor nodes. Since the position of each node in the network changes with time, the distance between any two nodes also changes dynamically. To evaluate the impact of dynamics on transmission, the interference prediction method is used to obtain the average interference value at each relay node [18]. Δt Represents the interference value at time t when the message is available at time t. $I(t|t_0)$ when is called the instantaneous interference value at time t. $t_0 = tI(t|t_c) = 0$ In a mobile scenario, the instantaneous obtained by () 0I t cannot well reflect the quality of the link within a period of time, and the average can well meet this requirement. Assuming that $f(x)$ and $g(x)$ respectively denote the link, gain function and attenuation function related to time t, the predicted interference at node a can be expressed as

$$I_a(t|t_0) = \sum_{j \neq a} \int_{t_0}^{t} g(x) f(x) dx \tag{2}$$

Using equation (2), the average of the link (a, e) can be obtained; when e is the transmitter node, and a is the receiver node, then:

$$\gamma_a^e(t|t_0) = \frac{g(x)f(x)}{v_0 + I_{a(t|t_0)}} \tag{3}$$

To simplify the representation, γ_a^e can be used instead of $\gamma_a^e(t|t_0)$. Using equation (3), the channel capacity from t_0 can be obtained as:

$$c_k(t) = w\ln(1+\gamma_a^e) \tag{4}$$

Where w represents the network bandwidth having a constant value. In the above equation, the link quality is expressed as the probability that the transmission rate of node e does not exceed the link capacity c_k. Assume that the path gain $|h_{ea}|^2$ obeys an exponential distribution with a variance σ2 =1; then, the rate interruption probability can be expressed as:

$$P_{ea}^{out} = 1 - \exp\left[-\frac{2^{\frac{\eta_k}{W}} - 1}{g_a^2}\right] \tag{5}$$

$$s_a^e = \frac{p_1 g x}{v_0 I_a}(t|t_0), \mu_e \tag{6}$$

According to equation (5), the link quality out can be obtained as:

$$U_{ea} = 1 - P_{ea}^{out} \tag{7}$$

3.1.2 QUEUING DELAY

Only the queuing delay is considered at each relay node. It is assumed that the data packets obey the exponential distribution with the mean value of K, and each node maintains a single queue. According to the calculation results, when the arrival process follows an independent exponential distribution, the expected queuing delay of link l at time t can be expressed as follows:

$$\bar{D}_k(t) = \frac{l}{C_k - \eta_k} \tag{8}$$

Where η_k and C_k represents the transmission rate and link capacity at time t.

3.1.3. QUEUING DELAY

To extend the usage time of the path and reduce the network resources consumed by reconstruction, each source node tries to adopt a path with a longer life cycle to transmit data streams. At time t_0, the coordinates of nodes e and a is given by:

$$L_e = \left(x_e^{t_0} + y_e^{t_0} + z_e^{t_0}\right) \tag{9}$$

$$L_a = \left(x_a^{t_0} + y_a^{t_0} + z_a^{t_0}\right) \tag{10}$$

The movement velocity vectors are expressed as:

$$\left(M_x^e + M_y^e + M_z^e\right) \tag{11}$$

$$\left(M_x^a + M_y^a + M_z^a\right) \tag{12}$$

According to the coordinates of nodes e and a at time t_v, the distance between them can be obtained as $d_{ea}^{t_v}$. If all nodes move in their respective directions at a constant speed within a specific time interval Δt time, then the coordinates of node e are:

$$L_e^{\Delta t} = \left(x_e^{t_0} + m_x^e \Delta t, y_e^{t_0} + m_y^e \Delta t, z_e^{t_0} + m_z^e \Delta t\right) \tag{13}$$

The coordinate e, Δt of node a after time Δt is calculated in the same way as the above equation.

According to and, the distance of two nodes after Δ*t* time can be obtained, when Δ*t* = *1*, If ae M is positive, the total distance between nodes e and a is $\Delta d_{ea}^{\ 1} = R - d_{ea}^{\ t0}$ if ea M is negative, the total distance is $\Delta d_{ea}^{\ 2} = d_{ea}^{\ t0} + R$ To sum up

$$d_{ea} = \begin{cases} \Delta d_{ea}^1, \bar{m}_{ea} > 0 \\ \Delta d_{ea}^2, \bar{m}_{ea} \leq 0 \end{cases} \tag{14}$$

According to the above equation and the separation rate ea M, the connection time of nodes e and a can be obtained as

$$CT_{ea} = \frac{\Delta d_{ea}}{|\overrightarrow{m}_{ea}|} \quad (15)$$

3.2. PROBLEM DESCRIPTION

To improve the network performance, the effective transmission rate $\tilde{r}_{ea}^{n}$ is used instead of the actual transmission rate r, where $r_{ea}{}^{n} = r_{klea}$. The use of larger transmission power for each transmission node can ensure the reliability of transmission and cause interference to other links. If there are more data streams in the network, this interference signal may prevent the receiver from receiving the data packets correctly. Therefore, controlling the transmission power of each transmitter can reduce interference to other data streams and improve link reliability while ensuring that data packets reach the base station within a given delay threshold. Since ACK messages are generally much smaller than data packets, the impact of ACK on transmission performance can be ignored. To express the path selection problem more intuitively, two variables need to be defined, which are as follow:

$$f_{ea}^{n} = \begin{cases} r_k^n, u_{ea} \\ 0 \end{cases} \quad (16)$$

$$\tilde{t}_{ea} = \begin{cases} t_{ea}^{i}, \tilde{r}_{ea}^{n} \neq 0 \\ 0, \tilde{r}_{ea}^{n} = 0 \end{cases} \quad (17)$$

Using the equations (16) and (17), the cross-layer optimization problem is expressed as:

$$min_{g} \sum_{e \in M} \sum_{a \in M} C(\tilde{r}_{ea}^{n}) + \sum_{e \in M} M(P_e) \quad (18)$$

$$S.t. \sum_{a \in m} \tilde{r}_{ea} \leq C_{kl}, \forall e \in M \quad (19)$$

$$\sum_{a \in m} \sum_{a \in m} \tilde{t}_{ea} \leq \zeta \quad (20)$$

$$P_{min} \leq P_e \leq P_{max}, \forall\, e \in M \quad (21)$$

Equation (18) is the joint cost function to minimize the cost function with effective transmission rate and power as parameters. Equation (19) ensures that the transmission rate used by each sender should not exceed the maximum capacity of the current link. According to equation (5), it can be seen that the quality of the link and the expected queuing delay is related to the transmission rate of the relay node. The speed can not only ensure the reliability of the link but also reduce the single-hop delay. Equation (20) indicates that the end-to-end delay consumed by each data stream should not exceed a given threshold; otherwise, the data packet will be relayed or discarded by the base station. Equation (21) limits the transmit power of the relay node to a certain range. It is necessary to ensure the reliability of transmission and reduce the interference to other data streams.

4. DISTRIBUTED SOLUTION

The centralized optimization method requires each node in the network to communicate with the control center to update the network parameters to get the optimal solution. The optimization method is not advisable in the fast-moving FANET of the node. On the one hand, the frequent exchange of information between nodes and the control center will consume substantial bandwidth and power resources, and concurrent transmission will cause interference to other links and reduce link quality. Centralized optimization requires the control center to receive the updated information sent by all nodes to perform the next step of optimization. In the case of poor link quality, the control center may take more waiting time for the information to be updated to the next node. The above two aspects determine that the centralized optimization method cannot be used in high-speed real-time transmission scenarios. The distributed method can address the limitations of the centralized method. Since it only requires the node to exchange updated information with its neighbor nodes to perform optimization operations. The proposed cross-layer optimization problem is non-convex, which can be converted into the convex optimization problem through the dual decomposition method.

The Lagrangian dual vector λ is introduced in equation (19). Each element *ea* λ in the vector corresponds to the constraint of a link. The problem can be transformed into

$$L(\tilde{r}_{ea}^{n}, P_e) = min\left\{ \sum_{e \in M} \sum_{a \in M} C(\tilde{r}_{ea}^{n}) + \sum_{e \in M} M(P_e) + \sum_{e \in M} \sum_{e \in M} \lambda_{ea} (\tilde{r}_{ea}^{n} - c_{ea}) \right\} \quad (22)$$

Recombine equation (22);

$$L(\tilde{r}_{ea}^{n}, P_e) = min\left\{ \sum_{e \in M} \sum_{a \in M} C(\tilde{r}_{ea}^{n}) + \lambda_{ea} \tilde{r}_{ea}^{n}) + \sum_{e \in M} \left(M(P_e) + \sum_{a \in M} \lambda_{ea} C_{ea} \right) \right\} \quad (23)$$

According to equation (23), the proposed cross-layer optimization problem can be divided into two sub-problems, as follows;

$$L^1(\tilde{r}_{ea}^{n}, \lambda) = min\left\{ \sum_{e \in M} \sum_{a \in M} C(\tilde{r}_{ea}^{n}) + \lambda_{ea} \tilde{r}_{ea}^{n} \right\} \quad (24)$$

$$L^2(P, \lambda) = min\left\{ \sum_{e \in M} \left(M(P_e) - \sum_{a \in M} \lambda_{ea} C_{ea} \right) \right\} \quad (25)$$

From equations (24) and (25), it can be seen that both sub-problems are convex optimization problems. Equation (24) optimizes real-time routing and rate allocation problems, while equation (25) optimizes power control problems. Both problems can be executed independently at each node using distributed methods.

Since the path delay constraints are globally coupled, all nodes included in the path must work together to make the end-to-end delay satisfy equation (20). The original decomposition method is used to divide equation (24) further to eliminate the global coupling constraint. An auxiliary vector y is introduced to transform the global constraint into a local constraint. Each term in y is related to the delay constraint on a single link. By considering the vector y, equation (24) can be transformed into:

$$min \sum_{e \in M} \sum_{a \in M} C(\tilde{r}_{ea}^{n}) + \lambda_{ea} \tilde{r}_{ea}^{n}) \quad (26)$$

$$s.t. \sum_{a \in M} \tilde{t}_{ea} \le y_{ea}, \forall e \in M \quad (27)$$

$$\sum_{e \in M} \sum_{a \in M} y_{ea} \le \zeta, \lambda_{ea} \ge 0 \quad (29)$$

If y_{ij} is regarded as the single-hop delay threshold on link one at time t, the optimization equation (26) can be divided into two sub-problems with each sending node e, the optimization goal is given by:

$$\min\left\{\sum_{a \in M} C(\tilde{t}_{ea}^{m}) + \lambda_{ea} \tilde{t}_{ea}^{R}\right\} \quad (30)$$

Assuming that $F^*(y)$ represents the optimal cost function of the problem equation (30) when the delay constraint vector y is used, the coupled delay constraint set y is updated by solving the following optimization form:

$$\min F^*(y)$$

$$s.t. \sum_{e \in M} \sum_{a \in M} y_{ea} \le \xi \quad (32)$$

Introducing the dual vector μ for the delay constraint in the problem equation (30), the problem is transformed into:

$$L^3(\tilde{t}_{ea}^{m}, \lambda, \mu) = \min\left\{\sum_{a \in M} (C(\tilde{t}_{ea}^{m}) + \lambda_{ea} \tilde{t}_{ea}^{R} + \mu_{ea}(\tilde{t}_{ea} - y_{ea}))\right\} \quad (33)$$

$$s.t.\ \lambda_{ea} \ge 0, \mu_{ea} \ge 0, \forall e, a \in M \quad (34)$$

Introducing the dual vector β into equation (31), we can get:

$$L^4(y, \beta) = \min\left\{F^*(y) + \left(\sum_{e \in M} \sum_{a \in M} \beta_{ea}\right)\left(\sum_{e \in M} \sum_{a \in M} y_{ea} - \xi\right)\right\} \quad (35)$$

Replace the left term with the term on the right side of the inequality, equation (35) becomes:

$$L^5(y, \beta) = \min\left\{F^*(y) + \sum_{e \in M} \sum_{a \in M} \beta_{ea} y_{ea} \sum_{e \in M} \sum_{a \in M} \beta_{ea}\right\} \quad (36)$$

βij is regarded as the maximum available delay time allocated to link l. If the vector y^* is the optimal solution of equation (35), then it must also be the optimal solution of equation (36), so $\sum_{v \in M} \sum_{u \in M} (\beta_{vu}\, \zeta_v) = \zeta$. Since □ is a constant, we can get $y_{vu} \le \beta_{vu}\, \zeta$, the prerequisite for formula (33) to obtain an optimal solution or a feasible solution is that the vector y used in formula (33) must be the optimal solution of formula (31) or at least a feasible solution $\sum_{e \subset M} \sum_{a \subset M} \beta_{ea} = 1$. Thus, the relationship between dual vectors μ and β in the two problems can be obtained; thus, $\sum_{e \in M} \sum_{a \in M} \mu_{ea}, y_{ea}$ and $\sum_{e \in M} \sum_{a \in M} \beta_{ea}, y_{ea}$ are equivalent. The solution obtained by formula (31) y^* can satisfy the constraint condition of (33). From equation (31), we can get an optimal solution y^*, then the dual form of the cross-layer optimization problem can be expressed as:

$$\max D(\lambda, \mu) = L^2(P, \lambda) + L^3(\tau^2, \lambda, \mu) \quad (37)$$

$$s.t.\ \lambda \ge 0, M \ge 0 \quad (38)$$

Using the traditional dual-based optimization method, the update operation of the vectors λ and μ in each iteration can be obtained as:

$$\lambda_{ea}(t+1) = [\lambda_{ea}(t) + \varepsilon \textstyle\sum_{a \in M} \tilde{t}_{ea} - C_k] \quad (39)$$

$$\mu_{ea}(t+1) = [\mu_{ea}(t) + \xi \textstyle\sum_{a \in M} \tilde{t}_{ea} - y_{ea}] \quad (40)$$

Where ε and ξ denote the step size of two update operations, respectively. Because the high-speed mobility of nodes in FANET leads to rapid changes in link connectivity, choosing a constant step size can ensure the convergence of the optimization problem and accelerate the convergence rate. According to the dual parameter values, the original parameters e, a, τ and P_e can be calculated as:

$$\tau_{ea}(t+1) \quad (41)$$

$$\arg\min\left\{\sum_{a \sim M} (C(\tilde{t}_{ea}^{m}) \mid \lambda_{ea}(t \mid 1) \tilde{t}_{ea}^{m} \mid M_{ea}(t \mid 1)(\tilde{t}_{ea} \quad y_{ea})\right\} \quad (42)$$

$$P_e(t \mid 1) = arg\ \min_{P_{min} \le P_e \le P_{max}}\left\{\sum_{e \sim M} (M(P_e) \mid \sum_{a \sim M} \lambda_{ea}(t \mid 1) C_{ea}\right\} \quad (43)$$

The solution presented above is only suitable for synchronization optimization scenarios because each iteration in the optimization process requires new parameter information. In FANET, the link quality is poor due to node mobility and signal interference. Data packets will be discarded because the total delay consumed is more significant than a given threshold. Synchronous optimization cannot work well in the scenarios mentioned above; thus, an asynchronous update method is used to optimize different network parameters to solve this problem. The asynchronous update method allows data packets to be lost during transmission, and nodes that have not received data packets can use their stored old information to update network parameters. Define variables $\tau_{ea}(t)$ and $\varsigma_{ea}(t)$ as the projection on the iteration sequence t, that is, the sequence number of the nearest iteration because each data packet has one delay threshold.

When the transmission delay consumed by some relay nodes is greater than the threshold, the relay node considers the current data packet as invalid and discards it. Then, the subsequent nodes can update it according to the stored old parameter information. In this way, $\tau_{ea}(t)$ and $\varsigma_{ea}(t)$ are used to replace the current iteration sequence$t$. If the relay node receives a data packet, then $\tau_{ea}(t) = t$ and $\varsigma_{ea}(t) = t$, update the operating formula (39). The sum in equation (40) can be modified as:

$$\lambda_{ea}(t+1) = [\lambda_{ea}(\tau_{ea}(t) + \varepsilon(\textstyle\sum_{a \subset M} \tilde{t}_{ea} - C_k)] \quad (44)$$

$$\mu_{ea}(t+1) = [\mu_{ea}(\varsigma_{ea}(t) + \xi(\textstyle\sum_{a \subset M} \tilde{t}_{ea} - y_k)] \quad (45)$$

To make the optimization problem to converge to the optimal solution, the average value of the current iteration t is used in the actual operation to replace the parameters τ_{ea} and P_e in equations (42) and (43), where

$\overline{r}_{ea} = \frac{1}{t}\sum_{v=1}^{t} r_{ea}(n)$ and $\overline{P}_e = \frac{1}{t}\sum_{v=1}^{t} P_e(n)$. Similar to the traditional routing method, the source node pre-establishes an end-to-end path for each data packet, and the lifecycle of this path is not determined but is related to the short connection time of the link on the path. Each node in the network that broadcasts routing request messages consumes a lot of unnecessary resources due to the location of the base station in FANET, which is usually fixed. Thus, certain specific methods need to be adopted to reduce resource consumption due to broadcasting. In the below equation, a variable SPP (single-hop packet progress) is defined that represents the distance gain of relay node j relative to its parent node i.

$$Spp = \hat{d}_e - \hat{d}_a \quad (46)$$

Where, $\hat{d}_e$ represents the distance from the node e to the base station. The set of available neighbors for each node is $A_e = \{(e,a) \in N \cap sp_{ea} > 0, \forall a \in M\}$. when node e receives routing request information, it only broadcasts this information to node e. In the path selection stage, each node uses the same rate and power to transmit request packets, so a routing index needs to be designed to enable the node to select the optimal path. Here the two constant weighting factors 1 ω and 2 ω, assume that the set of links that the data packet travels from the source node to e is e L, and the path utility at node e is;

$$Q_e = \omega_1 \min_{l \in L_e}\{CT_l\} - \frac{\omega_2}{H_e} \quad (47)$$

Among them, H_e is the number of hops from the source node s to the current node e. The delay-aware cross-layer optimization is implemented in two steps, including the meeting time.

The path selection algorithm description is illustrated in algorithm 1.

Algorithm 1 Path selection algorithm

1) //initialization
2) At relay node e
3) If node e receives the request packet for the first time
4) Each V_e^t node a
5) if $sp_{ea} > 0$
6) Add node a to A_e;
7) end if
8) end for
9) end if
10) Calculate CT_{se} and Q_e based on formula (8) and formula (33);
11) if $Q_e > Q_e$, then
12) $Q_e \leftarrow Q_e$ and save the parent node s;
13) else
14) Discard the data packet;
15) end if
16) if $CT_{se} < CT$ then
17) $CT \leftarrow CT_{se}$, ch ++;
18) end if
19) Node e broadcasts the data packet to each node in A_e
20) end if
21) At the destination node BS:
22) BS selects the path forwarding number with a large base station

The specific execution process and parameters of Algorithm 1 are described as follows. In the network initialization phase, each node e broadcasts a HI packet to its neighbors. When the neighbor node a receives the HI packet from node e, it returns a response packet containing its identifier and coordinates, and then node e extracts the information of a from the received response packet and saves it. If node e receives a path request packet from node s, it calculates CT_{se} and Q_e as per equations (15) and (47), respectively. If Q_e is greater than the value Q_e. Currently saved by V_e^t, replace this value with Q_e and record the transmission node in the routing table, otherwise discard the data packet. If CT_{se} is less than the existing CT in the packet header, replace this value with the current CT_{se} and add 1 to the transmission hop count ch^{++} value of the packet header. Then i broadcasts the path request packet to each node in i until the request packet reaches the base station. When the base station receives a path request message, it extracts min CT and HI from the request packet and uses equation (47) to calculate the total path utility $Q(BS)$. If $Q(BS)$ is greater than the currently saved value, then replace it with the new value and record the transmission node in the routing table; otherwise, the base station discards the request packet.

After reaching the end time of the route request, the base station sends a reply message to the node recorded in the routing table. Each relay node extracts and saves min CT from the reply packet and repeats this process until the reply message reaches the source node.

Through the above path establishment process, each selected node saves the information of the next-hop node and the small duration min CT of the path. Based on this information, the following optimization operation can be performed. Using the idea of distributed optimization, algorithm two is executed at each relay node e. Algorithm two does not require each node to have global optimization information, and each relay node only uses the received neighbor information to complete the optimization operation. To understand algorithm two more clearly, its execution process is described as follows.

The dual vectors λ and μ are initialized, and the set of relay nodes obtained by algorithm one is given simultaneously. When the relay node e receives the data packet at $t + 1 > CT_{min}$, it first judges whether the data packet has timed out at the current moment. The total transmission delay of the data packet exceeds a given threshold; node e discards the received data packet.

The stored local dual variables λea and μea use equations (5), (8), (42), and (43) to obtain the current transmission rate r and power Pe, and calculate the mean values of e, a, and Pe, respectively. If $t + 1 > CT_{min}$ node e clears the routing table and dual variables from the cache table, and then it will return to algorithm 1. Otherwise, node i will update the two dual variables according to equations (44) and (45) and saves them in the cache. Node e uses e, a, r and

Pe to pass the data packet to the next-hop node a, and repeat the step until the data packet reaches the base station. If some relay nodes do not receive data packets within the delay threshold $\Im$, they will update the dual variables with the relevant parameters stored before. This transmission task will end until the base station receives the data packet.

In the initialization phase, each node sends query packets to surrounding neighbor nodes to construct the network topology. The time complexity of this process is $O(|V|^2)$. For each node i, to obtain the set of available neighbors, node e refers to steps 3 to 7 in algorithm 1 to determine which neighbor nodes can be added to I. The time complexity is max ON. In step 8, node e calculates CT_{ai} and Q_e based on equations (15) and (47), and the time complexity is $O(1)$. Step 9 ~Step 16 are two judgment conditions, all of which can be completed in unit time. The time complexity can be expressedas $O(1)$. In step 17, node i broadcasts the path request packet to each node of i, and the time complexity is 0. To find the optimal cost path, node i may receive multiple path request packets from neighbors. If node i receives the path request packet for the first time, perform step 3 ~ step 19; otherwise, only perform step 10 ~step 19. Node e can receive V_{max}^2 path request data packets. The time complexity of step 10 ~ step 19 is $V_{max} = (O(1) + O(1) + O(1))$, which can be simplified to N_{max}^2. Step 3 ~ Step 19 are only executed once, so when the time complexity is V_{max}^2. The time complexity for all nodes in the network to execute algorithm 1 is OV_{max}^2, therefore, the time complexity $O|V^3|$ under bad conditions can be obtained. Combining the time complexity of initialization and the time complexity of path selection, the total time complexity of algorithm 1 is $O|V^3|$.

Algorithm 2. Asynchronous distributed cross-layer optimization (Case model 3)
1) At relay node e and its relay node a:
2) Init the parameters $\lambda_{ea}(0)$, $\mu_{ea}(0)$ and obtain the relay node j from the routing table;
3) Calculate the link capacity on formula (3); 4) if the current total delay t <□, then
5) Obtain μi from the packet header and calculate the remaining number H_r;
6) if $1-\mu_e \leq \mu_{ea}$, then
7) Update the dual variables λ_{ea} and μ_{ea} based on equations (30) and (31);
8) else $1-\mu_e$
9) $\mu_{ea} \leftarrow$;
10) Then use the λ_{ea} and μ_{ea} before the current (H_r) to update the dual variables;
11) end if
12) end if
13) Node e calc r_{ea} and p_e on formula (4), formula (5), formula (28) and formula (29);
14) Node e sends data packets to the relay node selected by algorithm 1
15) if t + >1 CT_{min}
16) Call algorithm 1;
17) End if

5. SIMULATION EXPERIMENT

In this study, the simulation and evaluation of the performance of the CASE MODEL 3 were carried out using the NS3 simulation. CASE MODEL 3 mainly considers queuing delay and transmission delay, while the delay caused by the MAC layer competition is ignored in the experiment, and the slotted-ALOHA protocol is used to realize the function of the MAC layer. All the UAVs are assumed to be evenly distributed in 1000 m × 1000 m, and the ground base station is fixed at the coordinates (700 m, 700 m). All UAVs have the same transmission radius of 250 m. When there is data packet transmission, the UAV sends data according to the optimized transmission rate and power layer, and the power value to be optimized is selected from the range [0.37 W, 0.66 W]. The generation of data streams in the network obeys the Poisson distribution with a parameter of 25, and the maximum delay of each data packet is ten hops. For the location information of the UAVs, GPS is installed on each UAV. All UAVs also have the location information of the base station.

The dual vector $\lambda(0)$ is initialized as the queuing delay of each link. If the number of path hops established in the route discovery phase is H, then $1(0) = iH\mu$ at each relay node. Also, the values of the two-step size factors in CASE MODEL 3 are compared with the CASE MODEL 1 (robust and reliable predictive). CASE MODEL 1 is a three-dimensional routing protocol proposed for FANET, which mainly considers connection time and end-to-end hop count, while CASE MODEL 2 does not consider routing issues. In CASE MODEL 1, the transmission rate of the node is 12 Mbit/s, the transmission power is 0.45 W, and the settings of other parameters are the same as mentioned above. The experimental results mainly include four parameters: time-out rate, packet loss rate, throughput, and energy consumption. These results are divided into two parts according to the difference in the moving rates and the number of nodes. Figures 2 to 5 show the comparison results of the four network parameters in the three methods under different mobile speeds. Figures 6 to 9 are the comparison results of the three methods under different numbers of nodes ε.

Figure 2 shows that as the mobile speed increases, the data packet-timeout rate of the three methods also increases. CASE MODEL 3 considers the end-to-end delay constraint. Before transmitting data packets, each relay node must evaluate the delay with its neighbors according to equation (8). CASE MODEL 2 allows the delay of data packets to be greater than the threshold within a certain range; thus, the relay node will discard these data packets. Also, CASE MODEL 3 provides better results than CASE MODEL 2 under strict end-to-end delay conditions. The packet-timeout rate of DNUM is low. To obtain an optimal solution to the optimization problem, the relay node selects the neighbor to meet the current delay constraint as the next-hop node. Since CASE MODEL 1 does not consider the end-to-end delay constraint. Thus, the relay node it selects may consume more time to transmit data packets. Also, the delay constraint is evaluated at each relay node, CASE MODEL 3 and CASE MODEL 2 have a lower timeout rate than CASE MODEL 1, as shown in picture 2. An increase in the movement rate results in a shorter connection time. The transmission between two nodes may fail because they move out of each other's

communication range, which consumes more time delay. Therefore, the timeout rate varies for the three methods, i.e., gradually increase as the speed of movement increases.

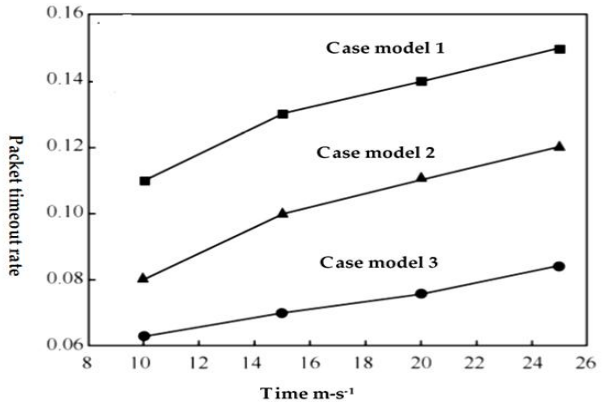

Figure 2. Packet timeout rate of the three routing methods under different mobile speeds

The total packet loss rate includes the timeout rate and the packet loss rate caused by exceeding the number of retransmissions at the relay node. In CASE MODEL 3, each relay node evaluates the link quality with its neighbors according to equation (5). The quality is optimized as a parameter in the objective function. The optimal transmission rate obtained by equation (42) also implies the current good link quality, while the use of a fixed transmission rate in CASE MODEL 1 may result in poor link quality. Therefore, CASE MODEL 2 and CASE MODEL 1 will spend more transmission times at the relay node than CASE MODEL 3, resulting in a greater packet loss rate. CASE MODEL 2 also does not consider link quality issues. Only optimizing the transmission rate does not guarantee the reliability of transmission. Therefore, the total packet loss rate of CASE MODEL 2 is greater than that of CASE MODEL 3. As shown in Figure 3, CASE MODEL 3 has a lower total loss rate than CASE MODEL 2 and CASE MODEL 1. Generally, the lower the total loss rate, the more data packets received by the destination node, and the higher the network's throughput. Therefore, CASE MODEL 3 has higher throughput than CASE MODEL 2 and CASE MODEL 1, as shown in Figure 4.

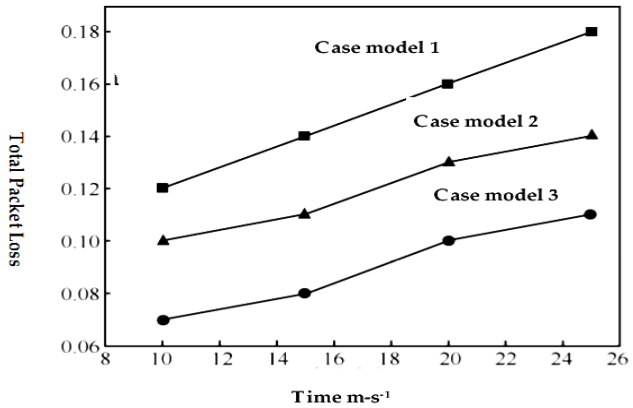

Figure 3. The total packet loss rate of the three routing methods under different mobile speeds

To reduce the interference between signals and improve the reliability of end-to-end transmission, CASE MODEL 3 requires each relay node to calculate the current optimal power layer according to equation (43). The optimal power obtained through equation (43) can reduce the interference between signals and, at the same time, improve the link quality. Thus, the relay node can complete the end-to-end transmission with fewer retransmission times. On the other hand, CASE MODEL 2 and CASE MODEL 1 uses a fixed power layer, resulting in poor link quality at higher data flow. Moreover, retransmissions at each relay node mean more energy consumption; thus, CASE MODEL 3 consumes less energy to transmit a single data packet than CASE MODEL 2 and CASE MODEL 1, as shown in Figure 5.

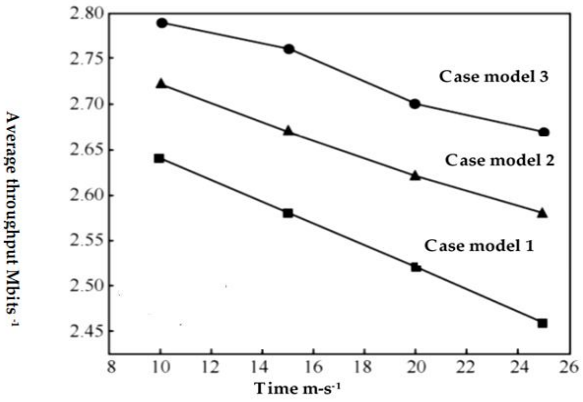

Figure 4. Average throughput of the three routing methods under different mobile speeds

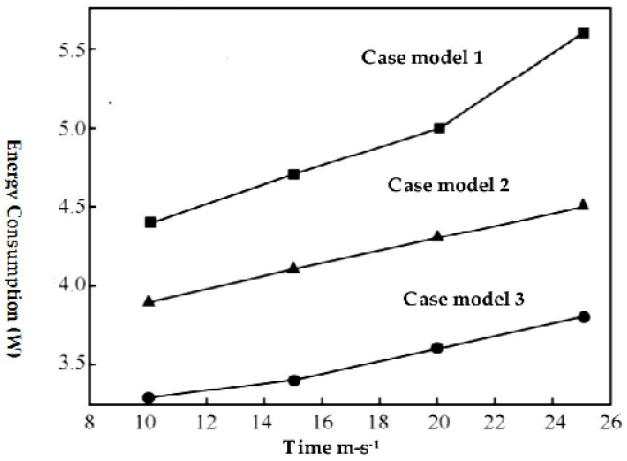

Figure 5. Energy consumption in the three routing methods under different mobile speeds

Figure 6 to 9 shows the results of the three different models at node's moving speed (15 m/s). It can be seen from Figure 6 that when the number of nodes in the network increases, the timeout rates of the three methods decreases. Due to the end-to-end delay constraints, the smaller the total number of nodes, the fewer next-hop nodes the relay node can choose. In poor link quality, the relay node may spend more time delaying one-hop transmission, which increases the probability of data packet timeout. When the number of nodes in the network is extensive, each relay node can select

neighbors with better link quality to transmit data packets. On the other hand, a more significant node density means a longer connection time, and the probability of data packet loss due to multiple transmission times becomes smaller. Therefore, as the number of nodes increases, the total loss rate of a model decreases.

CASE MODEL 3 takes into account both the end-to-end delay and the link quality; thus, it has a lower total packet loss rate than CASE MODEL 1 and CASE MODEL 2 (which only considers end-to-end delay), as shown in Figure 7. Similar to the previous analysis, the lower the total packet loss rate, the higher the throughput. From Figure 8, it can be seen that CASE MODEL 3 has higher throughput than CASE MODEL 2 and CASE MODEL 1 under the different number of nodes. The joint consideration of the rate and power optimization improves the network's throughput and reduces the interference between signals and the number of single-hop retransmissions. It can be seen from Figure 9 that at different nodes, CASE MODEL 3 consumes less energy to complete end-to-end transmission than CASE MODEL 2 and CASE MODEL 1.

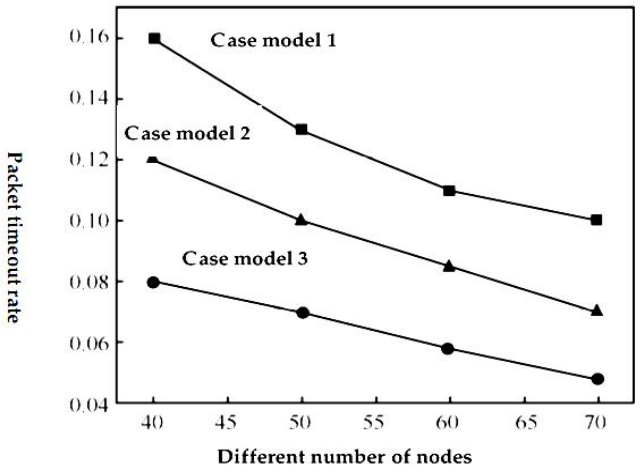

Figure 6. The packet-timeout rate of the three routing methods under different numbers of nodes

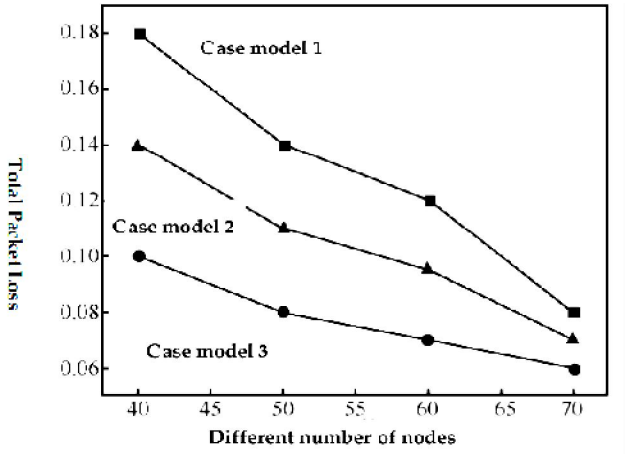

Figure 7. The total packet loss rate of the three routing methods under different numbers of nodes

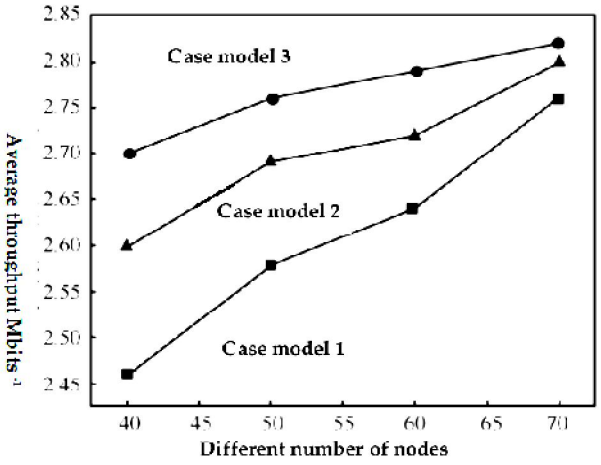

Figure 8. The average throughput of the three routing methods under different numbers of nodes

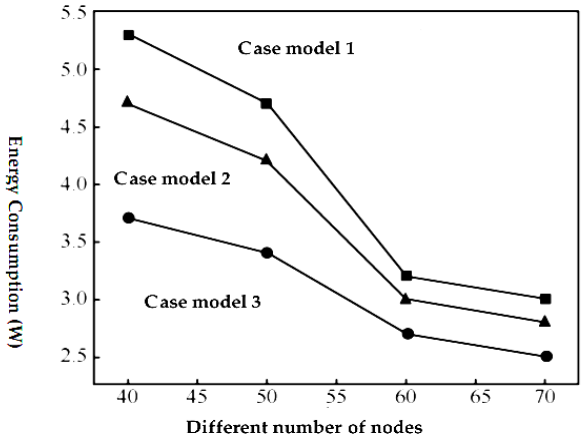

Figure 9. Energy consumption of the three routing methods under different numbers of nodes

6. CONCLUSIONS

This paper proposes a delay-aware distributed cross-layer optimization method CASE MODEL 3, which solves the problems of real-time routing, rate allocation, and power control by dividing the optimization process into two steps. To realize the distributed solution, the cross-layer optimization problem is first formalized as a non-convex optimization problem, and then the Lagrangian relaxation technique is used to eliminate the non-convex constraints. The dual decomposition method is then used to decompose a global problem into two sub-problems, and the original decomposition method is used to eliminate the global coupling delay constraint. Considering the unreliability of the wireless link, the original and dual parameters are updated using the idea of the asynchronous update until the algorithm reaches the optimal solution or a given update interval. The experimental results show that the CASE MODEL 3 has good performance regarding throughput, energy consumption, and timeout rate. The proposed method requires that the set of available neighbors of all nodes cannot be empty. In the future, the problem of empty nodes and how they influence the performance of the FANET should be investigated.

ACKNOWLEDGEMENT

This work is idea of authors and supervisor. Authors thanks to the reviewers and editor of journal for constructive comments.

REFERENCES

1. Duan, B.; Fang, S.; Zhu, R.; Wu, X.; Wang, S.; Gong, Y.; Peng, Y. Remote estimation of rice yield with unmanned aerial vehicle (UAV) data and spectral mixture analysis. Front. Plant Sci.2019, 10, 1–14, doi:10.3389/fpls.2019.00204.
2. Derakhshandeh, S.Y.; Mobini, Z.; Mohammadi, M.; Nikbakht, M. UAV-Assisted Fault Location in Power Distribution Systems: An Optimization Approach. IEEE Trans. Smart Grid2019, 10, 4628–4636, doi:10.1109/TSG.2018.2865977.
3. Zhang, H.; Song, L.; Han, Z.; Poor, H.V. Cooperation Techniques for a Cellular Internet of Unmanned Aerial Vehicles. IEEE Wirel. Commun.2019, 26, 167–173, doi:10.1109/MWC.2019.1800591.
4. Chriki, A.; Touati, H.; Snoussi, H.; Kamoun, F. FANET: Communication, mobility models and security issues. Comput. Networks2019, 163, 106877, doi:10.1016/j.comnet.2019.106877.
5. Cheng, S.; Feng, Y.; Wang, X. Application of Lagrange relaxation to decentralized optimization of dispatching a charging station for electric vehicles. Electron.2019, 8, doi: 10.3390/electronics8030288.
6. Chang, T.H.; Hong, M.; Liao, W.C.; Wang, X. Asynchronous Distributed ADMM for Large-Scale Optimization - Part I: Algorithm and Convergence Analysis. IEEE Trans. Signal Process.2016, 64, 3118–3130, doi:10.1109/TSP.2016.2537271.
7. Zhang, J.; You, K. Fully Asynchronous Distributed Optimization with Linear Convergence in Directed Networks. 2019, 2, 1–14.
8. Li, X.; Huang, J. ABPP: An adaptive beacon scheme for geographic routing in FANET. In Proceedings of the Parallel and Distributed Computing, Applications and Technologies, PDCAT Proceedings; IEEE, 2018; Vol. 2017-Decem, pp. 293–299.
9. Khan, M.A.; Safi, A.; Qureshi, I.M.; Khan, I.U. Flying ad-hoc networks (FANETs): A review of communication architectures, and routing protocols. In Proceedings of the 2017 1st International Conference on Latest Trends in Electrical Engineering and Computing Technologies, INTELLECT 2017; IEEE, 2018; Vol. 2018-Janua, pp. 1–9.
10. Qu, S.; Zhao, L.; Xiong, Z. Cross-layer congestion control of wireless sensor networks based on fuzzy sliding mode control. Neural Comput. Appl.2020, 32, 13505–13520, doi: 10.1007/s00521-020-04758-1.
11. Wu, D.; Yang, T.; Stoorvogel, A.A.; Stoustrup, J. Distributed Optimal Coordination for Distributed Energy Resources in Power Systems. IEEE Trans. Autom. Sci. Eng.2017, 14, 414–424, doi:10.1109/TASE.2016.2627006.
12. Rukmani, K. V.; Nagarajan, N. Enhanced channel allocation scheme for cross layer management in wireless network based on interference management. Cluster Comput.2019, 22, 9825–9835, doi: 10.1007/s10586-017-1596-7.
13. Xu, J.; Xu, X.; Ding, X.; Shi, L.; Lu, Y. Wireless recharging sensor networks cross-layer optimization based on successive interference cancellation. IEICE Trans. Commun.2020, E103B, 929–939, doi:10.1587/transcom.2019EBP3218.
14. Farazi, S.; Klein, A.G.; Brown, D.R. Age of Information with Unreliable Transmissions in Multi-Source Multi-Hop Status Update Systems. In Proceedings of the Conference Record - Asilomar Conference on Signals, Systems and Computers; IEEE, 2019; Vol. 2019-Novem, pp. 2017–2021.
15. Kennouche, T.; Cadoux, F.; Gast, N.; Vinot, B.; Asynchronous, A.; Kennouche, T.; Cadoux, F.; Gast, N. ASGriDS: Asynchronous Smart-Grids Distributed Simulator. In Proceedings of the In 2019 IEEE PES Asia-Pacific Power and Energy Engineering Conference (APPEEC); IEEE, 2019; pp. 1–5.
16. Aoudia, F.A.; Gautier, M.; Magno, M.; Gentil, M. Le; Berder, O.; Benini, L. Long-short range communication network leveraging LoRa™ and wake-up receiver. Microprocess. Microsyst.2018, 56, 184–192, doi:10.1016/j.micpro.2017.12.004.
17. Jiang, Y.; Liu, Q.; Zheng, F.; Gao, X.; You, X. Energy-Efficient Joint Resource Allocation and Power Control for D2D Communications. IEEE Trans. Veh. Technol.2016, 65, 6119–6127, doi:10.1109/TVT.2015.2472995.
18. Cong, Y.; Zhou, X.; Kennedy, R.A. Interference prediction in mobile ad hoc networks with a general mobility model. IEEE Trans. Wirel. Commun.2015, 14, 4277–4290, doi:10.1109/TWC.2015.2418763.